

Distinct behaviors of suppression to superconductivity in $LaRu_3Si_2$ induced by Fe and Co dopants

Sheng Li, Jian Tao, Xiangang Wan, Xiaxin Ding, Huan Yang and Hai-Hu Wen*

Center for Superconducting Physics and Materials,

National Laboratory of Solid State Microstructures and Department of Physics, Nanjing University, Nanjing 210093, China

In the superconductor $LaRu_3Si_2$ with the Kagome lattice of Ru, we have successfully doped the Ru with Fe and Co atoms. Contrasting behaviors of suppression to superconductivity is discovered between the Fe and the Co dopants: Fe-impurities can suppress the superconductivity completely at a doping level of only 3%, while the superconductivity is suppressed slowly with the Co dopants. A systematic magnetization measurements indicate that the doped Fe impurities lead to spin-polarized electrons yielding magnetic moments with the magnitude of $1.6 \mu_B$ per Fe, while the electrons given by the Co dopants have the same density of states for spin-up and spin-down leading to much weaker magnetic moments. It is the strong local magnetic moments given by the Fe-dopants that suppress the superconductivity. The band structure calculation further supports this conclusion.

PACS numbers: 74.20.Rp, 74.70.Dd, 74.62.Dh, 65.40.Ba

I. INTRODUCTION

Superconductivity in the systems RT_3Si_2 or RT_3B_2 (R stands for the rare earth elements, like La, Ce, Y, etc., T for the transition metals, like Ru, Co and Ni, etc.) is very interesting because it concerns the conduction of the d-band electrons of the 3d- or 4d- transition metals. By having different combinations of chemical compositions, one can tune the system from a superconducting (SC) ground state to a magnetic one, and sometimes have both phases coexisting in one single sample.^{1,2} The $LaRu_3Si_2$ has a SC transition temperature at about 7.8 K.^{3,4} Since the superconductivity is at the vicinity of the magnetic order, some unconventional pairing mechanisms, such as the charge fluctuation⁵, or anti-ferromagnetic spin fluctuations⁶ mediated pairings are possible. Recently, we find that both the superconducting state and the normal state exhibits some anomalous properties, suggesting that the electronic correlation plays important roles in the occurrence of superconductivity.⁷ Another reason for doing research on this system is that it may have some odd pairing symmetries, such as d -wave, $s+d$, $p_x + ip_y$ or $d_{x^2-y^2} + id_{xy}$,^{8,9} because the electric conduction is dominated by the 4d band of Ru atoms which construct a Kagome lattice (a mixture of the honeycomb and triangular lattice, as shown in Fig.1). Furthermore, the electric conduction in this system is strongly favored by the Ru-chains along the z-axis, as evidenced by our band structure calculations, this may induce quite strong superconducting fluctuations.⁷

In a superconductor, the impurity induced pair breaking depends strongly on the structure of the pairing gap and the feature of the impurities, such as magnetic or non-magnetic. Therefore it is very important to measure the impurity induced scattering effect in the superconducting state of $LaRu_3Si_2$. According to the Anderson's theorem,^{10,11} in a conventional s-wave superconductor, nonmagnetic impurities will not lead to apparent pair-breaking effect. This theoretical ex-

pectation has been well illustrated in the conventional superconductors.¹² However, a magnetic impurity, due to the effect of breaking the time reversal symmetry, can break Cooper pairs easily. In sharp contrast, in a d-wave superconductor, nonmagnetic impurities can significantly alter the pairing interaction and induce a high density of states (DOS) due to the sign change of the gap on a Fermi surface. This was indeed observed in cuprate superconductors where Zn-doping induces T_c -suppression as strong as other magnetic disorders, such as Mn and Ni.^{13,14} In $LaRu_3Si_2$, preliminary experiment indicated that the SC transition temperature drops only 1.4 K with the substitution of 16 % La by Tm (supposed to possess a magnetic moment of about $8\mu_B$), suggesting that the superconductivity is robust against the local paramagnetic moment¹. This kind of doping is induced at the sites of the rare earth elements, which may give very weak pair breaking effect on the Cooper pairs (3d electrons of Ru). Therefore it is very interesting to investigate what will happen if we dope impurity atoms directly to the Ru sites. In this paper, we report the doping effect on the Ru sites by the Fe and Co dopants. We find a contrasting suppression effect to the superconductivity with these two kind of dopants. Possible reasons are given to explain this effect.

II. EXPERIMENTAL METHODS AND CHARACTERIZATION

The samples of $La(Ru_{1-x}T_x)_3Si_2$ ($T=Fe$ and Co) were fabricated by the arc melting method.^{1,3,4,7} The starting materials: La metal pieces (99.9%, Alfa Aesar), Fe powder (99.99%), Co powder (99.99%), Ru powder (99.99%) and Si powder (99.99%) were weighed, mixed well, and pressed into a pellet in a glove box filled with Ar (water and the oxygen compositions were below 0.1 PPM). In order to avoid the formation of the $LaRu_2Si_2$ phase, we intentionally add a small amount of extra Ru powder (about 15% more) in the starting materials. Three

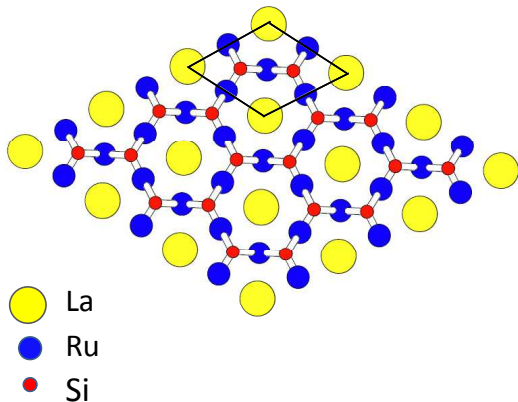


FIG. 1: (color online) Top view of the atomic structure of LaRu_3Si_2 . The Ru atoms construct a Kagome lattice (blue middle size circles), while the Si (red small size circles) and La atoms (yellow large size circles) form a honeycomb and a triangle structure, respectively. The three different atoms don't overlap each other from a top view. The prism at the top corner illustrates one unit cell of the structure.

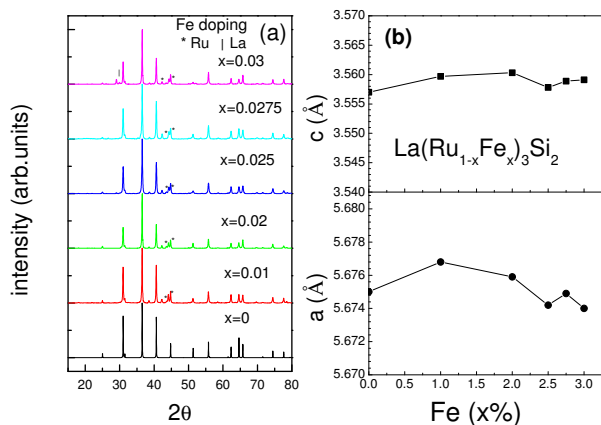


FIG. 2: (color online) (a) X-ray diffraction patterns of the sample $\text{La}(\text{Ru}_{1-x}\text{Fe}_x)_3\text{Si}_2$. One can see that the main phase is the 132 structure, with slight Ru impurity phase. (b) Doping dependence of the a -axis and c -axis lattice constants. Because Fe doping is only up to 3%, so there is no distinct change of the lattice constant.

rounds of welding with the alternative upper and bottom side of the pellet were taken, in order to achieve the homogeneity. The X-ray diffraction (XRD) measurement was performed on the Brook Advanced D8 diffractometer with $\text{Cu K}\alpha$ radiation. The analysis of XRD data was done with the softwares Powder-X and Fullprof. The resistivity and magnetization measurements were done on the Quantum Design physical property measurement system (PPMS-16T) and SQUID-VSM.

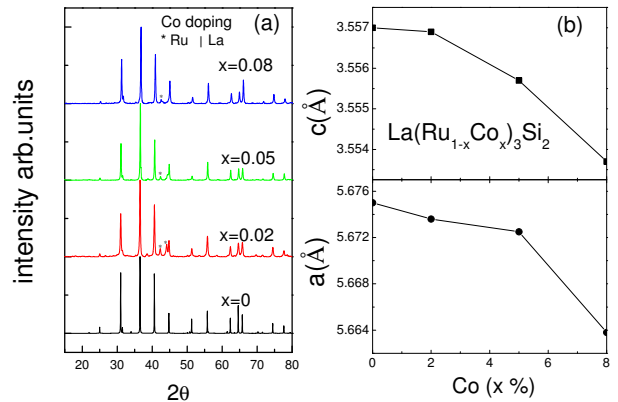


FIG. 3: (color online) (a) X-ray diffraction patterns of the sample $\text{La}(\text{Ru}_{1-x}\text{Co}_x)_3\text{Si}_2$, up to the doping level of 8% the sample is still quite clean. (b) Doping dependence of both a and c lattice constants with the increase of doped Co concentration.

The XRD patterns for Fe- and Co-doped samples are shown in Fig.2 and Fig.3, respectively. One can see that the samples are rather clean, except for a small amount of Ru impurity. For the Fe-doped samples, we don't see clear change of the lattice constant a and c . This could be due to two reasons: (1) The maximal doping level here is 3% which is already enough to kill the superconductivity completely; (2) The atoms of Fe and Ru are in the same column and close to each other in the periodic table, we would assume that the ions of Fe and Ru have the similar radii. For the Co-doping, however, there is an obvious decrease of a and c lattice constant with doping, as shown in Fig.3. The variation of the lattice constants in the Co-doped samples are well associated with the resistivity data shown below, clearly suggesting that the Co atoms are also successfully doped into the LaRu_3Si_2 system.

III. RESULTS AND DISCUSSION

A. Suppression to superconductivity

In Fig.4(a) and (b), we present the temperature dependence of the normalized resistivity of Fe- and Co-doped samples. It can be seen that the transition temperature was suppressed remarkably with Fe-doping, and shifted to below 2 K at only a doping level of 3%. However, for the Co-doped ones, there is no significant change of T_c , up to 8% Co-doping. These behaviors are also revealed by the magnetization of the samples, as shown in Fig.4(c). For the superconducting samples, the resistivity increases monotonously with the increase of doping level, both for the Fe and Co doping. But it is clear that, the enhancement of the residual resistivity, although weaker

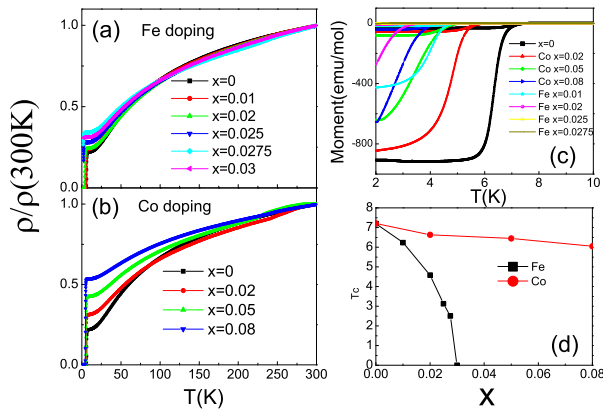


FIG. 4: (color online) (a) Temperature dependence of normalized resistivity with Fe doping, there is no superconducting transition with the doping level at only 3%. Slightly enhancement of the residual resistivity is observed, indicating an enhanced scattering. (b) Temperature dependence of the normalized resistivity with Co doping, the suppression to the superconducting transition by Co doping is rather weak. (c) Temperature dependence of DC susceptibility of the $\text{La}(\text{Ru}_{1-x}\text{T}_x)_3\text{Si}_2$ ($T=\text{Fe}$ and Co) under $H = 50$ Oe, measured in the zero-field-cooled (ZFC) and field-cooled (FC) processes. (d) Doping dependence of T_c in Fe- and Co-doped samples, the suppression to T_c in Fe doped samples is drastically fast, but that by Co doping is very slow.

in the Fe-doped samples than that in the Co-doped ones, but the suppression to the superconductivity is the opposite. In Fig. 4(d) we illustrate the suppression of T_c with doping concentrations of Fe and Co. This is easy to be understood in the way that, the suppression to the superconductivity in the Fe-doped samples is induced by the local magnetic moments. These magnetic scattering centers are detrimental to the Cooper pairs, and thus suppress the superconducting transition temperature significantly. However, in the normal state these impurities, although possessing strong magnetic moments, act as the usual scattering centers. In the Co-doped case, the increase of the residual resistivity is quite strong. For example, the residual resistivity increases more than 100 % with the Co doping level of about 8%. However, the superconducting transition temperature drops only about 2 K. This sharp contrast between the behaviors of the Fe and Co-doped samples is unexpected from a straightforward picture, since both Fe and Co would behave similarly, i.e., both would contribute local magnetic moments and influence the electric conduction, as well as the superconductivity.

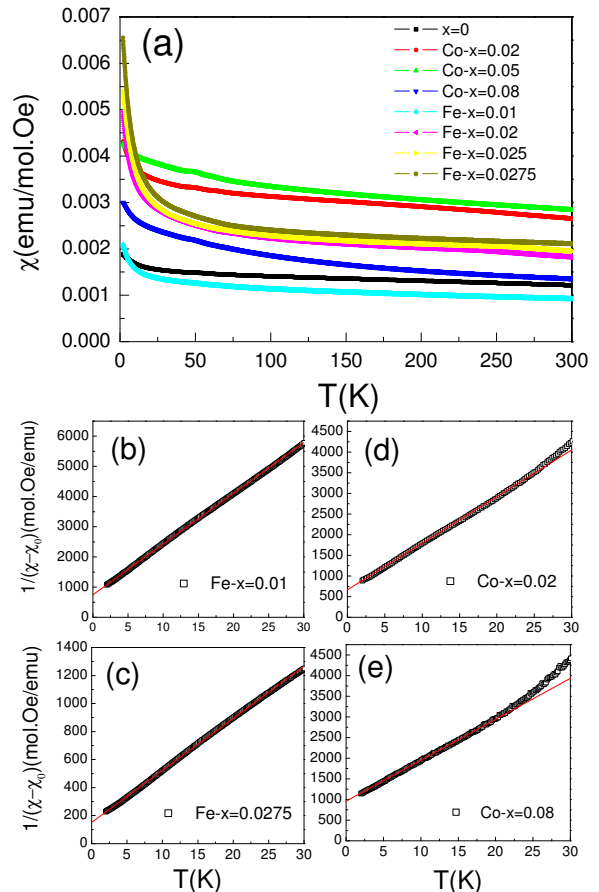


FIG. 5: (color online) (a) Temperature dependence of DC magnetic susceptibility for Co and Fe doped samples under 3 T. A low-T diverging is observed for the Fe-doped samples, indicating an doping induced local magnetic moments. (b)-(e) The fit to the low temperature data yielding the magnetic moments (see Table I).

B. Doping induced magnetic moments

In order to unravel the puzzle concerning the sharp contrast between the Fe and Co-doped samples, we have done the magnetization measurements under high magnetic fields. The raw data of magnetization measured at 3 T up to room temperature are shown in Fig.5(a). The temperature dependence of the magnetic susceptibility look similar, however, it is only for the Fe-doped samples, that there is a diverging of the magnetic susceptibility at low temperatures. This diverging of χ at low temperatures can be understood as the formation of some strong local magnetic moments. The magnetization for Co-doped samples reveals an itinerant moment. To illustrate this point more clearly, we fit the low temperature magnetization with the Curie-Weiss law,

$$\chi = \chi_0 + C/(T + T_0), \quad (1)$$

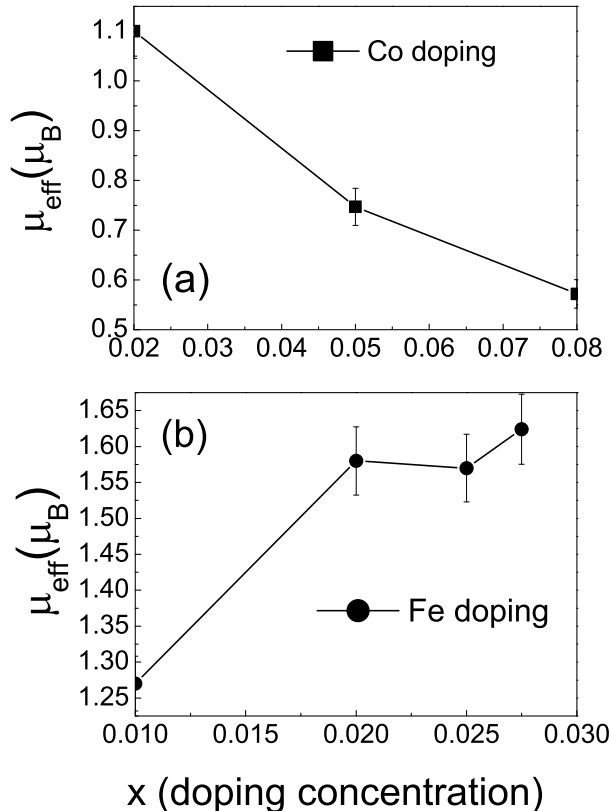


FIG. 6: (color online) Magnetic moment with Fe and Co doping calculated by the constant C in the Curie-Weiss law (eq.1). (a) The doped Fe impurities lead to an enhanced magnetic moment. (b) The Co doping gives a gradually weakened magnetic moment.

TABLE I: Fitting parameters with Curie-Weiss law for the Co- and Fe-doped samples.

doping	$C(K \cdot emu/mol \cdot Oe)$	$T_0(K)$	$\mu_{eff}(\mu_B)$
Co-0.02	0.00883	5.596	1.1
Co-0.05	0.01046	12.608	0.747
Co-0.08	0.00984	9.307	0.572
Fe-0.01	0.00613	4.553	1.27
Fe-0.02	0.0188	5.097	1.58
Fe-0.025	0.02304	4.89	1.57
Fe-0.0275	0.02723	4.628	1.624

where $C = \mu_0 \mu_{eff}^2 / 3k_B$, χ_0 and T_0 are the fitting parameters. The first term χ_0 arises mainly from the Pauli paramagnetism of the conduction electrons, the second term is induced by the local magnetic moments, given by the doped ions. In order to derive the correct values for C and χ_0 , we adjust χ_0 value to make the $1/(\chi - \chi_0)$ vs. T as a linear relation in the low temperature limit, the slope gives $1/C$, and the intercept delivers the value of

T_0 . The data treated in this way is shown in Fig.5(b)-(e). Here Fig.5(b) and Fig.5(c) are representing results for the Fe-doped samples with $x = 0.01$ and $x = 0.0275$; Fig.5(d) and Fig.5(e) are for the Co-doped ones for $x = 0.02$ and $x = 0.08$. One can see that the low temperature part is indeed linear. Once C is determined, we can get the magnetic moment given by the Fe and Co ions μ_{eff}/Co or μ_{eff}/Fe . It turns out that $\mu_{eff}/Co = 0.572\mu_B$ in the Co-doped ($x=0.08$) sample, $1.62\mu_B/Fe$ in the Fe-doped one ($x = 0.0275$). Fig.6(a) and Fig.6(b) show the derived μ_{eff} for Co- and Fe-doped samples, respectively. The decrease of the μ_{eff} in Co-doped samples indicates the weakening of the magnetic moments compared to the parent sample, which suggests that the density of states of spin up and spin down contributed by the Co atoms are equal. This is also consistent with the theoretical results: Co-dopant introduces negligible magnetic moments. While in Fe-doped samples, an increase of μ_{eff} is observed showing the enhancement of magnetic moments by the Fe impurities. This strongly suggest that the electrons given by the Fe ions are more polarized, yielding a magnetic moment of about $1.6\mu_B/Fe$, comparable to the theoretical calculation: $2.05\mu_B/Fe$.

It is interesting to mention that, although the Ru and Fe are in the same column in the periodic table, the doped Fe atoms apparently play a very different role as the Ru does. This is consistent with the common sense that the 3d electrons (here contributed by Fe ions) are more localized leading to the magnetic moments. This is very different from that in the iron pnictide superconductors in which many different kind of 3d or 4d transition metals can be doped to the Fe sites for inducing superconductivity, showing a wide flexibility.¹⁵⁻¹⁹ Doping many transition metals, like Co, Ni, Pd, Ir, Pt and Ru does not induce very strong magnetic moments, instead the antiferromagnetic order is suppressed. On the other hand, in $LaRu_3Si_2$, doping Co does not suppress the superconductivity quickly, although the impurity scattering is strong. This effect manifests that the pairing gap is probably s-wave type, although gap anisotropy exists for the present system.⁷ It remains to be explored that whether the Co-doping in $LaRu_3Si_2$ can result in a "dome" like doping dependence of superconducting transition temperature, or in other words, can we find an antiferromagnetic (AF) order as the parent phase and superconductivity can be induced by suppressing this AF order.

C. Density-functional theory calculations

Using WIEN2k package²⁰, we studied the electronic structure based on the generalized gradient approximation.²¹ To consider the low doping concentration, we perform calculation for a $2 \times 2 \times 2$ supercell, and replace one of the 48 Ru atoms in the supercell by Fe/Co. In Fig.7, we show the Fe/Co 3d partial DOS. It is interesting to find that the main part of Co 3d is located below E_F . Therefore Co 3d band is close to fully

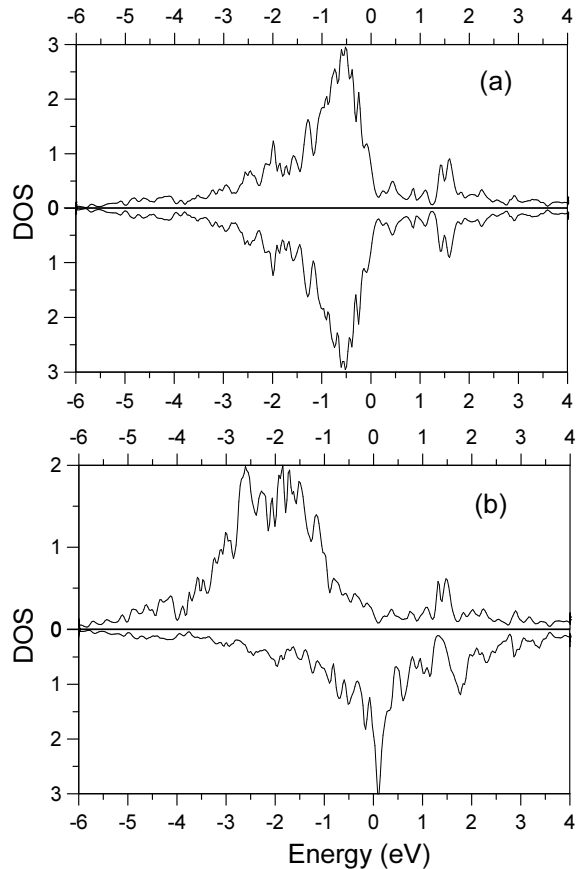


FIG. 7: (color online) Calculated 3d partial DOS, (a) for Co 3d orbitals; (b) for Fe 3d orbitals. The positive and negative value signal the spin up and spin down portion of the DOS.

occupied, although due to the hybridization with Si and Ru, Co 3d has also distribution above Fermi level (E_F). Thus, it is natural to expect that the spin splitting is

very small, and Co becomes nonmagnetic as shown in Fig.7(a). For Fe, while the spin-up channel is almost fully occupied like Co, the spin-down is clearly partially occupied as shown in Fig.7(b). Therefore, there is a big exchange splitting and the magnetic moment at Fe-site is found to be $2.05 \mu_B$, close to our experimental value $1.6 \mu_B$. Because of the strong hybridization with Fe 3d electrons, the neighboring Ru-site has also about $0.1 \mu_B$ magnetic moment.

IV. SUMMARY

In summary, contrasting behaviors of the suppression to superconductivity has been observed in Fe and Co doped LaRu_3Si_2 . In the case of doping Fe, the superconductivity can be easily suppressed, while it is much slower in the Co-doped samples. Measurements and analysis on the DC magnetization suggest that the Fe-doping induce some strong local magnetic moments, while Co-doping does not. This is well consistent with our DFT calculations. In the Fe-doped samples, the impurities act as strong pair breakers, which is caused by the local magnetic moment. While the doping of Co atoms brings about equally spin-up and spin-down electrons which contributes negligible magnetic moment. Therefore the pair breaking is much weaker in the Co-doped samples.

Acknowledgments

We appreciate the useful discussions with Jan Zaanen, Zidan Wang, and Jianxin Li. This work is supported by the NSF of China (11034011/A0402), the Ministry of Science and Technology of China (973 projects: 2011CBA00102 and 2012CB821403) and PAPD.

* hhwen@nju.edu.cn

* Electronic address: hhwen@nju.edu.cn

¹ M. Escorne, A. Mauger, L. C. Gupta and C. Godart, Phys. Rev **B49**, 12051 (1994).

² H. C. Ku *et al.*, Solid State Comm. **35**, 91 (1980).

³ H. Barz, Mater. Res. Bull. PNAS **15**, 1489 (1980); J. M. Vandenberg and H. Barz, *ibid.* **15**, 1493 (1980).

⁴ C. Godart and L. C. Gupta, Phys. Lett.**120**, 427 (1987).

⁵ U. Rauchschwalbe, W. lieke and F. Steglich *et al.*, Phys. Rev. **B30**, 444 (1984).

⁶ D. J. Scalapino, Phys. Rep. **250**, 329 (1995). T. Moriya and K. Ueda, Rep. Prog. Phys. **66**, 1299(2003). P. Monthoux, D. Pines and G. Longarich, Nature **450**, 20 (2007).

⁷ Sheng Li, Bin Zeng, Xiangang Wan, Jian Tao, Fei Han, Huan Yang, Zhihe Wang, and Hai-Hu Wen, Phys. Rev. **B84**, 214527(2011).

⁸ Qiang Han, D.Wang, Qiang-Hua Wang, and Tianlong Xia,

Phys. Rev. Lett. **92**, 027004 (2004).

⁹ Jing Kang, Shun-Li Yu, Zi-Jian Yao and Jian-Xin Li, J. Phys. Condens. Matter **23**, 175702 (2011).

¹⁰ P. W. Anderson, J. Phys. Chem. Solids **11**, 26 (1959).

¹¹ For a review on the impurity effect on superconductivity, one is referred to A. V. Balatsky, J. X. Zhu, I. Vekhter, Rev. Mod. Phys. **78**, 373 (2006).

¹² A. Yazdani, B. A. Jones, C. P. Lutz, M. F. Crommie, and D. M. Eigler, Science **275**, 1767 (1997).

¹³ S. Pan, *et al.* Nature **403**, 746(2000).

¹⁴ G. Xiao *et al.*, Phys. Rev. **B42**, 8752 (1990).

¹⁵ A. S. Sefat, R. Y. Jin, M. A. McGuire, B. C. Sales, D. J. Singh, and D. Mandrus, Phys. Rev. Lett. **101**, 117004 (2008).

¹⁶ C. Wang, Y. K. Li, Z. W. Zhu, S. Jiang, X. Lin, Y. K. Luo, S. Chi, L. J. Li, Z. Ren, M. He, H. Chen, Y. T. Wang, Q.

- Tao, G. H. Cao, and Z. A. Xu, Phys. Rev. B **79**, 054521 (2009).
- ¹⁷ N. Ni, S. L. Bud'ko, A. Kreyssig, S. Nandi, G. E. Rustan, A. I. Goldman, S. Gupta, J. D. Corbett, A. Kracher, P. C. Canfield, Phys. Rev. B **78**, 014507 (2008).
- ¹⁸ Fei Han, Xiyu Zhu, Ying Jia, Lei Fang, Peng Cheng, Huiqian Luo, Bing Shen and Hai-Hu Wen, Phys. Rev. **B80**, 024506 (2009).
- ¹⁹ Shilpam Sharma, A. Bharathi, Sharat Chandra, Raghavendra Reddy, S. Paulraj, A. T. Satya, V. S. Sastry, Ajay Gupta, C. S. Sundar, Phys. Rev. **B81**, 174512 (2010).
- ²⁰ P. Blaha, K. Schwarz, G. Madsen, D. Kvasnicka, and J. Luitz, WIEN2k, An Augmented Plane Wave + Local Orbitals Program for Calculating Crystal Properties (Technical University of Vienna, Vienna, 2001).
- ²¹ J. P. Perdew, K. Burke, and M. Ernzerhof, Phys. Rev. Lett. **77**, 3865 (1996).